Up-scaling nanoparticle synthesis by sputter deposition in ionic liquids

Michael Meischein
Ruhr-Universität Bochum: Ruhr-Universitat Bochum
Alfred Ludwig (alfred.ludwig@rub.de)
Ruhr-Universität Bochum: Ruhr-Universitat Bochum https://orcid.org/0000-0003-2802-6774

Research Article

Keywords: ionic liquids, sputter deposition, copper nanoparticles, upscaling nanoparticle synthesis

Posted Date: April 13th, 2021

DOI: https://doi.org/10.21203/rs.3.rs-321433/v1

Abstract

Up-scaling of nanoparticle fabrication by sputtering into an ionic liquid is shown for the example of Cu. Long-time sputtering (24 h) into a large amount (50 mL) of the ionic liquid 1-butyl-3-methylimidazolium bis-(trifluoromethylsulfonyl)imide [Bmim][$(Tf)_2N$] yields an amount of approximately 1 g Cu nanoparticles (mean spherical diameter (2.6 ± 1.1) nm), stabilized in ionic liquid without agglomerations. Extraction of Cu nanoparticles from the stabilizing ionic liquid was performed with the capping agent hexadecylamine. Extracted particles could be redispersed in other solvents, thus enabling applications of sputtered nanoparticles beyond ionic liquids.

1. Introduction

Metallic nanoparticles (NPs) have many application possibilities, e.g. in medicine (Breisch et al. 2019; Conde et al. 2012; Weissleder et al. 1990), optics (Li and Zhang 2009), electronics (Karmakar et al. 2011) and catalysis (Astruc 2008; Kharisov et al. 2019; Migowski and Dupont 2007). For applications, an effective large-scale synthesis process of nanoparticles is necessary. NPs are most frequently prepared by wet chemical approaches comprising the reduction or decomposition of metal precursors (Bracey et al. 2009; Garzón-Manjón et al. 2015; Garzón-Manjón et al. 2018a; Itoh et al. 2004; Raut et al. 2009; Sahoo et al. 2009; Yang et al. 2009) , but also mechanical techniques like milling or attrition (Baraton 2003; Datta et al. 2000) can be used, representing bottom-up and top-down methods for NP synthesis. In literature, several publications exist concerning NP synthesis enabling an upscaling of the NP yield to the gram level. Besides mechanical processes like ball milling (Lam et al. 2000), chemical or thermal decomposition of precursors (Cui et al. 2009; Kim et al. 2015; Lee et al. 2005; Lee et al. 2008; Lee and Chen 2006; Song and Chen 2003; Wen et al. 2012) and (flame) spray synthesis (Athanassiou et al. 2006; Wang et al. 2020) are commonly used for a high yield of NP amounts. Upscaling synthesis of NPs using ionic liquids (ILs) was also reported (Lu et al. 2009; Xiao et al. 2013; Zheng et al. 2009).

The unique physical and chemical characteristics of ILs makes them an interesting medium for chemical and industrial processes, for example in catalysis (Luska et al. 2015) and as reaction and scavenging media (Plechkova and Seddon 2008). ILs consists only of special structured cations and anions. They can be regarded as liquid salts at temperatures < 100°C. Taking all suitable cations and anions for IL synthesis into account, 10^{18} ILs could be fabricated (Holbrey and Seddon 1999), serving as a vast pool for different applications and task-specific design of individual ILs. In general, ILs possess outstanding characteristics making them versatile media for NP synthesis. Their negligible vapor pressure (Kuwabata et al. 2014; Wasserscheid and Keim 2000) provides the application of ILs as green chemistry solvents and clean substrates for vacuum processes (Vekariya 2017).

Wet chemical NP synthesis routes can be applied in ILs and comprise a huge part of the literature dealing with large-scale NP synthesis. One drawback of those reactions are chemical byproducts which can be present in the resulting colloidal solution, which can impede applications of the NPs (Torimoto et al. 2006).

Overcoming these drawbacks by avoiding precursor chemicals and their decomposition products can be achieved by physical vapor deposition (PVD) of metals in ILs (Richter et al. 2010, 2011). Thermal evaporation

for NP synthesis in ILs has been applied (Richter et al. 2011), but shows the drawback of necessary high thermal energies depending on the evaporation temperatures of the used elements. Additionally, for fabrication of binary NPs, the different specific vapor pressures of the elements makes the adjustment of a desired alloy composition challenging (König et al. 2014). Sputter deposition of metals into pure ILs is a PVD technique for fabrication of custom- and task-designed NPs with adjustable size and morphology, controlled by the used IL, and multinary composition without byproducts or organic impurities (Hatakeyama et al. 2009; Torimoto et al. 2006). The NP formation occurs without any stabilization agents and the composition of binary or multinary NPs can be determined by co-sputtering and the specific sputter rates of the elements controlled by the applied sputtering powers (Hirano et al. 2013; König et al. 2014). The (multinary) NP formation by sputtering into ILs is not limited to reaction mechanisms and the availability of precursor chemicals since all vacuum compatible chemical elements can be used as target materials for (co-)sputtering (König et al. 2014; Meischein et al. 2019; Meyer et al. 2018).

However, it is commonly believed that sputtering is not a suitable technique for synthesizing NPs in a large scale (Lam et al. 2000). However, there are reports which applied sputtering for a potential up-scaled synthesis of NPs, contradicting this assumption. For example, sputtering of Au on a powder substrate resulted in well-dispersed NPs, representing a synthesis technique showing scalability and no waste stream (Veith et al. 2005). Since the potential of sputtering for large-scale NP synthesis was indicated in literature and since sputter deposition in ILs is a powerful and versatile synthesis tool for NP production, we aimed to increase the obtained NP amount over the usual scientific scale (usually a few) by an extended sputter deposition of Cu into the IL [Bmim][$(Tf)_2N$]. We increased the IL amount and the deposition time and decreased the distance from the target to the receiving IL with respect to our usual sputter parameters in order to increase the sputter rate (Garzón-Manjón et al. 2018b; König et al. 2014; Löffler et al. 2018; Meischein et al. 2019; Meischein et al. 2020; Meyer et al. 2018). With this special experimental set-up we show the appropriateness of sputtering into ILs as a large-scale NP synthesis method.

The capping agent hexadecylamine (HDA) is used for extracting the Cu NPs out of the stabilizing IL. By addition of the capping agent to the Cu NP suspension, which is commonly used as stabilization mechanism in NP synthesis methods (Meshesha et al.), the NPs precipitate due to strong interactions of the HDA with Cu surrounding the NP surface and forming a surfactant cage around the individual NPs. The extremely low solubility of HDA in the IL, caused by the long apolar alkyl chain, leads to precipitation of the capped NPs out of the IL, ending as flocculated powder at the bottom of the reaction vessel. The HDA capped Cu NPs could be dissolved back into non-polar solvents or used for further investigations (König et al. 2014). TEM investigations of the as-sputtered and HDA-capped, re-dissolved NPs proof the success of the upscaled synthesis process, resulting in well distributed NPs in ILs. Inductively coupled plasma mass spectroscopy (ICP-MS) was used to determine the amount of metal in the extracted powder and in the sputtered IL to prove if a sufficient amount of material for up-scaling can be stabilized as NPs in ILs.

2. Methods And Materials

The sample synthesis process was started by sputtering of Cu into IL for the NP formation, followed by the Cu precipitation process using HDA as capping agent and the extraction of the precipitated Cu NPs from the NP/IL suspension.

2.1 Up-scaled sputter synthesis of Cu NP in IL

As liquid “substrate” for the sputter deposition of the NPs, the IL 1-butyl-3-methylimidazolium bis-(trifluoromethylsulfonyl)imide [Bmim][$(Tf)_2N$] was used. This IL was purchased from Iolitec (Heilbronn, Germany) with purity > 99%, halides content < 100 ppm and water content 51 ppm. Without further purification the IL was stored and processed under Ar atmosphere in a glovebox (water and oxygen content both < 0.5 ppm). A commercial co-sputter system (AJA POLARIS-5 from AJA INTERNATIONAL, Inc., North Scituate, MA, USA) with 1.5-inch diameter magnetron sputter cathodes and multiple sputter source DC power supplies (DC-XS 1500 from AJA INTERNATIONAL, Inc., North Scituate, MA, USA) was used for all sputter depositions. The process gas was Ar (purity 99.9999%, Praxair, Düsseldorf, Germany). A 38.1 mm diameter 3.175 mm thick Cu target (purity 99.99%, EvoChem, Offenbach am Main, Germany) was used.

For the up-scaled deposition, 50 mL of the IL [Bmim][$(Tf)_2N$] were filled into a clean petri dish (110 mm inner diameter 20 mm height) inside the glovebox. Prior to the deposition, the IL was evacuated inside the sputter chamber for 96 h in order to remove remaining water and oxygen from the transport out of the glovebox into the sputter chamber. The chamber pressure was Pa before the deposition. For plasma ignition, the chamber pressure was set to 1.33 Pa. After plasma ignition the target was pre-cleaned for 120 s at 20 W sputter power with a closed shutter in front of the target, a rotation of the substrate plate of 30 rotations per minute and a successive reduction of the Ar pressure to the deposition pressure of 0.5 Pa.
Pre-cleaning of the target was performed for removing possible oxide layers (Meyer et al. 2018), followed by adjusting the deposition power to 30 W (405 V, 75 mA) and opening the shutter in front of the cathode for the specific deposition time. To reach the total deposition time of 24 h, the deposition was conducted over three days with 9 h, 9 h and 6 h sputtering time per day. Between the depositions the sputter chamber was continuously pumped when the sputter gas line was closed after each deposition to achieve that the vacuum never exceeded the sputter pressure during the deposition processes. The cathode was tilted by an angle of 18° between the normal of the IL surface and the target normal. The distance between the IL surface and the cathode was decreased from 11 cm (standard) to 9 cm by placing another pair of petri dishes below the IL filled dish. A homogeneous deposition was achieved on the substrate due to rotation and cathode tilt. After the deposition, right after opening the chamber, 300 of the sputtered Cu NP/IL suspension were separated from the IL dish and transferred into the glovebox for storage and TEM sample preparation of the untreated IL. The remaining Cu IL volume was filled into a glass bottle and kept in air since for the capping procedure acetonitrile was used for washing the IL and thus a transfer into the glovebox would not be possible.

Subsequent to the deposition in IL, the sputter rate was determined using the identical sputter system configuration and deposition parameters (except deposition time) as for the IL deposition. The rate was determined using Si/SiO_2 pieces photolithographically structured with a photoresist lift-off cross pattern for film thickness measurements, also placed on a closed pair of petri dishes. The deposition time was 30 minutes to guarantee a sufficient film thickness. After deposition, the pieces were stored for 4 h in technical acetone to remove the lift-off photoresist and cleaned afterwards with technical acetone (purity 99.5%) and isopropanol (purity 99.7%). The film thicknesses was measured with a profilometer on 27 measurement points revealing a Cu deposition rate of 0.143 nm/s for this chamber configuration, which is approximately 80% higher than the usual Cu rate (0.08 nm/s) used in our standard scientific chamber configuration (Meischein et

al. 2019). For the synthesis parameters of the latter Cu NPs obtained from a scientific sputter deposition (used for comparison issues) see Meischein et al. (Meischein et al. 2019).

2.2 Capping of Cu NPs using HDA as capping agent

Acetonitrile (purity 99.5% from Fisher Scientific UK, Loughborough, England) was added to the Cu/IL suspension until both liquid phases had the same height in the bottle. Then, HDA (purity > 95.0%, from TCI Deutschland GmbH, Eschborn, Germany) was continuously added to the mixture with increasing single portions for slowly starting the NP capping and precipitation process (see Fig. 1). After each addition of capping agent (HDA), the IL acetonitrile mixture was stirred at 1500 rpm for 48 h. With increasing amount of HDA, the strength of the color of the remaining Cu IL decreases (Fig. 1(c)). A color change from brown to green of IL and capped NPs occurs due to the reaction of Cu with oxygen and water since all addition and stirring cycles were performed in air. For extracting all Cu NPs from the IL and obtaining a transparent IL phase above the NP phase, a total amount of 80 g HDA had to be used.

2.3 Extraction of HDA-capped Cu NPs

Extraction of the HDA-capped Cu NPs from the IL/acetonitrile mixture was achieved by centrifugation. The whole amount of IL/acetonitrile mixture was filled into centrifuge tubes (total volume 50 mL) so that each tube was filled with 35 mL. The rest of the volume was filled with fresh acetonitrile. After that, the tubes were shaken so that both liquid phases were mixed. The centrifugation was conducted using a Sigma 4-16S centrifuge (from Sigma Laborzentrifugen GmbH, Osterode am Harz, Germany) operated at 8000 rotations per minute, corresponding to a relative centrifugal force (rcf) of 10375 g. After the first centrifugation cycle of 2 minutes, the mixture of slight yellow/green colored IL/acetonitrile mixture above the capped Cu NPs at the bottom of the tubes was removed with a syringe and filled back into the container with the IL/acetonitrile mixture. This was done to ensure that the NP material, which was not capped by the HDA, was not lost during extraction. The tubes were refilled with new acetonitrile and were shaken again as long as the capped NPs were re-dissolved homogeneously in the tube volume. The centrifugation process was conducted again for the second to forth cycle. After a total of 4 cycles with consecutive removal and disposal of the remaining (clear) IL/acetonitrile mixture above the capped NPs, the remaining wet Cu NP powder from each centrifugation tube was mixed into acetonitrile and left in an open container overnight so that the acetonitrile could evaporate. The remaining HDA-capped and dried Cu NP powder was weighed for determining the extracted NP amount using the measured Cu metal content evaluated by ICP-MS.

2.4 TEM sample preparation

For the preparation of TEM samples holey carbon-coated Au grids (200 mesh, Plano GmbH, Wetzlar, Germany) were used. For the untreated as-sputtered Cu IL, 2.5 suspension was dropped on the carbon-coated grid side and left at this side for adhesion of the NPs for 2.5 h. In order to prevent possible grid contamination originating from interaction of the electron beam with the IL during TEM analysis, the grids were washed dropwise with dried acetonitrile for 1 h under inert conditions (see supporting information of Meyer et al. (Meyer et al. 2018)) and then stored in Ar atmosphere.

For the TEM investigations of the HDA-capped Cu NPs a spatula tip of the centrifuged powder was filled under air in an Eppendorf cap with toluene (purity 99.5 %, from VWR International GmbH, Darmstadt, Germany) and treated in an ultrasonic bath for 2 minutes. After the treatment in the ultrasonic bath, the powder was completely dissolved in toluene, resulting in a homogeneous green color of the beforehand colorless liquid, proving the successful re-dispersion of the HDA-capped Cu NPs into an apolar solvent. A few drops of the obtained mixture were filled into a new Eppendorf cap and were mixed with more toluene. This dilution was necessary to reduce the amount of HDA remaining on the TEM grid. A few drops of the obtained final solution were dropped on the carbon-coated side of the TEM grid and left for evaporation of the toluene inside a fume hood. Conventional TEM and high-resolution TEM (HRTEM) studies were performed using a FEI Tecnai F20 S/TEM instrument operated at 200 kV. For the analysis of the Cu NP mean diameter, at least 253 NPs were evaluated manually.

2.5 ICP-MS measurements

For ICP-MS measurements an amount of two times 50 of the Cu IL and an amount of 13.5 mg of the dried Cu NP powder obtained from the centrifugations were separated in suitable Teflon containers. To ensure a correct volume of IL separated into the containers, each container with the respective IL inside was additionally weighed. For the Cu IL, weighs of 54.7 mg in the first loaded and 69.6 mg in the second loaded container were measured. The differences between first and second loaded container may be due to the dry pipette tip during the first loading since the viscosity of the IL prevents the complete loading and unloading of the adjusted IL volume in the used Eppendorf pipette tip. The separated samples were diluted each with 4 mL of 69% concentrated phosphoric acid of the “ROTIPURAN® Supra” line. These mixtures were chemically digested in a Multiwave Pro microwave digestion device with 8-slot container holder 8NXF100 (Anton Paar GmbH, Graz, Austria). The digestion occurred at maximum temperature 240°C and maximum pressure 60 bar to ensure a complete transfer of the investigated material into solvable nitrides which could be measured in the ICP-MS. The resulting solutions were further diluted with ultrapure water (conductivity 0.055 /cm) to a total volume of 10 mL per sample. From this stem-solutions, 1:100- and 1:1000-dissolutions were produced and experienced an acidification with 2% phosphoric acid prior to the measurements in an iCAP RQ ICP-MS device (from Thermo Fisher Scientific Inc., Waltham, Massachusetts, USA). The ICP-MS measurements were conducted in the KED-mode to decrease disturbances from molecule ions.

3. Results

The results are presented in a TEM part, confirming the existence of NPs in the sputtered ILs as well as the extracted powder and a general analysis part of the Cu NP extraction in terms of necessary capping agent, obtained extracted material and its metal content determined by ICP-MS.

3.1 TEM results of the NPs obtained from the ILs and the extracted powder

As-prepared and HDA-treated ILs were analyzed by TEM to confirm the existence of Cu NPs in the IL and the HDA/IL/acetonitrile mixture. The TEM data of the Cu NPs obtained from the up-scaled sputtering in IL were compared with TEM data of Cu NPs synthesized with our standard procedure (Meischein et al. 2019) for scientific investigations. Fig. 2 shows TEM images of Cu NPs obtained from the up-scaled synthesis Cu/IL

directly after the deposition. The main amount of the NPs is organized in group structures where the individual NPs are close together. Crystallinity of the NPs was confirmed by the FFT data of the NPs depicted in the HRTEM image insets.

Cu NPs synthesized with our standard protocol for scientific purposes are shown in Fig. 3, again directly after sputter deposition in IL. These NPs show a very uniform distribution on the TEM grid and bigger NPs with respect to the up-scaled-synthesis NPs shown in Fig. 2. For both deposition types, the NPs show the fcc crystal structure as analyzed by the respective FFT data.

Furthermore, the size distributions of the NPs are comparable, as shown in Fig. 4. In both NP systems the highest number of NPs has a diameter of 2 nm, followed by 3 nm diameter. Additionally, the mean diameters are comparable. For the up-scaled deposition, a NP mean diameter of nm was evaluated which is in good agreement with the mean diameter of nm for the “scientific deposition”.

The comparison between the HDA-capped Cu NPs in Fig. 5 and the as-prepared Cu NPs from the up-scaled deposition in Fig. 2 shows that the HDA capping separated the NPs from each other and prohibited the formation of the agglomeration of Cu NPs. However, for both sample conditions, single NPs have been found in TEM investigations, with sizes around 2 nm.

3.2 General analysis of the extracted Cu NP powder

For the final state of the extraction procedure depicted in Fig. 1 (g), a total amount of 80 g HDA had to be used for extracting all of the NP material and leaving the IL nearly transparent. The centrifugation resulted in a total amount of capped NPs of approximately 139.32 g. During the precipitation procedure no agglomeration and precipitation of the NPs besides when capping with HDA was observed, as depicted in the image series of Fig. 1. Only the brown/green HDA-capped Cu NPs segregate out of the liquid IL, but no other segregates have been discovered. The liquid phase above the capped NPs becomes more and more transparent with increased HDA addition, but the homogeneous color indicates that the NPs stay stabilized in the IL matrix without own agglomeration.

The ICP-MS revealed a Cu weight proportion of 0.922% for the 50 Cu IL and 0.818% for the 13.5 mg of the dried and centrifuged Cu/HDA powder. Projected on the whole sputtering process, the total IL volume of 50 mL would contain 0.66 g of sputtered Cu (using the assumption of 1.44 g/cm³ for the IL density as outlined by the IL delivering company) and the whole centrifuged powder 1.14 g.

4. Discussion

The aim of this study was to clarify the question, if an up-scaled synthesis of NPs in IL could be achieved by sputter deposition. According to literature, a NP weight in the double digit gram regime can be regarded as large-scale NP synthesis (Cui et al. 2009; Lam et al. 2000; Song and Chen 2003). From the deposition rate and time one can calculate the nominal film thickness of a Cu film deposited on the IL surface. The comparison of our up-scaled Cu deposition with the Cu deposition for scientific purposes shows some interesting differences (see table 1) in terms of the obtained sputtered film and the IL loaded with NPs.

Deposition	Deposition rate (nm/s)	Deposition time (s)	Film thickness (m)	Diameter IL surface (mm)	Calculated film weight (g)	IL volume (mL)	Cu concentration in IL (mol/L)
Up-scaled	0.143	86400	12.364	110	1.05	50	0.3313
“Scientific”	0.080	7200	0.576	6	0.000146	0.035	0.0656

Table 1: Comparison of the deposition parameters and sample holder characteristics of the up-scaled and the scientific Cu deposition in IL. The sample holders for both deposition types are designed so that the IL volume is cylindrical with circular IL surfaces. For comparison issues, only one cavity of the cavity array plate used as sample holder for the scientific depositions has been considered.

The calculated film thickness with the information of the IL surface diameter results in a calculated upper weight limit of Cu sputtered into the IL. In the case of the up-scaled synthesis, a Cu amount of approximately 1 g is deposited on and into the IL. Since there was no agglomeration of the Cu material in the IL volume the amount of 1 g Cu is assumed to be stabilized as well-distributed NPs in the IL (see Fig. 2). Additionally, the size distributions of the up-scaled and the scientific depositions show a good agreement concerning mean diameter and general NP sizes, also indicating no relevant quality difference of the up-scaled and scientific synthesized ILs.

The ICP-MS results support this assumption. For the up-scaled Cu deposition, a Cu amount of 0.66 g in the IL and of 1.14 g in the extracted powder was extrapolated. The discrepancies of the respective metal amounts in the measured ILs from the calculated values may be explained by the pipetting and weighing of the ILs, since always a small amount of IL stays in the pipette tip and since the high viscosity of the IL complicates the incorporation of exact 50 from the container into the pipette and from there into the Teflon container for the chemical digestion. The Cu amount extrapolated from ICP-MS results for the centrifuged HDA/Cu powder is in agreement with the calculated Cu amount deposited into the IL and lies within a tolerance of 10% error.

Although the Cu metal concentration in the up-scaled-synthesized IL is five times higher than the Cu metal concentration in the scientific synthesis IL, well dispersed and non-agglomerated NPs are obtained in both cases. For the up-scaled synthesis, the concentration of sputtered material in the ILs is now a parameter to estimate if the NPs stay well-dispersed in the stabilizing IL matrix without agglomerations. Most publications report on NPs in ILs synthesized with methods other than sputtering with concentrations in the range of our scientific IL (Richter et al. 2011; Salas et al. 2011; Zhang et al. 2012). Also, concentrations in the range of our up-scaled IL (Qadir et al. 2018; Qadir et al. 2019) and a concentration higher than in our up-scaled IL was reported (with an small additive of IL-like ions originating from the IL synthesis process, see supporting information of Dash and Scott) (Dash and Scott 2009). Those results show, that NP concentrations even higher than our obtained concentration are possible without uncontrolled or unwanted NP agglomeration. The absence of the formation of a Cu film on the IL surface and the missing of unwanted Cu agglomerations within the uninfluenced IL after the depositions reveals that the stabilization ability of the IL was not exceeded by our up-scaled synthesis. Therefore, the amount of stabilized NPs in IL can be enlarged easily, since we sputtered with a relatively small cathode for a limited time into a limited volume of IL. For example, sputtering with more than one cathode would increase the sputtering rate by the number of the used cathodes and thus

lead to more NP material due to a nominally thicker “virtual” film. Sputtering from bigger cathodes would also increase the deposition rate since (i) the target area exposed to the sputtering Ar gas is bigger and (ii) the applied sputtering power can be increased for bigger targets since the maximum power before damaging the target increases with the target area and volume. Finally, if the used IL volume is increased, also more NPs can be stabilized. Due to the current available technical equipment it would be possible to design sputtering systems with a consecutive IL supply from ambient pressure to required sputter pressures in the sputtering area. A possible schematic design of an up-scaled product unit is shown in Fig. 6.: an IL assembly line where the IL is (purified and) loaded on the line in Ar atmosphere, pumped down over several consecutive pumping stations to the sputter pressure and is released after sputtering again to an Ar (or any other suitable inert) atmosphere at ambient pressure for storing and packing the IL product.

The quality of the obtained NPs shows no relevant differences concerning shape and distribution with respect to NPs synthesized for scientific purposes. The up-scaled-synthesized NPs exist in the as sputtered and the HDA-capped state as individual, non-agglomerated particles, as proven by the TEM investigations. However, in the HDA-capped state, the NPs have a smoother and more regular distribution as in the as prepared state. This distribution is attributed to the HDA capping agent, which is extracting the capped NPs out of the IL. The comparable long apolar alkyl chain of the HDA prevents physical contact of the NPs and contributes to a comparable uniform distribution over the TEM grid, since the chains at one capped NP also serve as distance keepers to the surrounding capped NPs.

By extracting the Cu NPs from the IL with the HDA capping agent, more applications become possible, e.g. if ILs were not an appropriate solvent for the desired process catalyzed by the NPs. The capped NPs can be easily dissolved back into apolar solvents as shown by the successful solvation into toluene, increasing the pool of suitable solvents for the NP colloids.

Since either NPs in IL can be used for their desired applications within the stabilizing IL or the NPs could be extracted by chemical routes, the obtained up-scaled-synthesized NP amount can be used for a various number of applications now with industrial scales.

5. Conclusion

Sputtering was applied for an up-scaled synthesis of Cu NPs in IL. The comparison of Cu NPs obtained from the up-scaled synthesis route with Cu NPs obtained from scientific preparation protocols shows only subtle differences although the material concentration in the up-scaled IL is five times higher than in the scientific IL. The extraction of the Cu NPs obtained from the up-scaled synthesis by addition of HDA as capping agent was performed for showing an alternative way of NP stabilization as well as demonstrating that those NPs can be used in different solvents than in ILs. The result of about 1 g of stabilized Cu NPs from sputtering in IL with special parameters but in a comparable small IL volume using a small cathode with low sputtering power shows the suitability of sputter deposition into ILs for large-scale NP synthesis when using scaled synthesis machines and parameters.

Declarations

Funding: This work was funded by the BMBF project NEMEZU and the German Science Foundation (DFG) via the project LU1175/23-1.

Conflict of interest: The authors declare that there is no conflict of interest.

Availability of data and material: Not applicable.

Code availability: Not applicable.

Authors' contributions: Michael Meischein conducted the sample synthesis, the sample processing, the TEM sample analysis, the NP size determination, all experiments except those mentioned in the acknowledgements and wrote the manuscript. Alfred Ludwig provided funding, scientific supervision and discussion, validation and manuscript writing, review and editing. All authors have read and agreed to the published version of the manuscript.

Ethics approval: Not applicable.

Consent to participate: Not applicable.

Consent for publication: Not applicable.

ACKNOWLEDGMENTS

We want to thank Florian Lourens for assistance in literature review concerning nanoparticle upscaling. Additionally, we want to thank the Center of Electrochemical Sciences (CES) at the Ruhr-University Bochum for (i) granting access to their centrifuge and Dr. Patrick Wilde for his introduction into the centrifuge operation and (ii) for conducting the ICP-MS measurements operated by Martin Trautmann. CES: Chair for Analytical Chemistry, Center for Electrochemical Sciences, Faculty of Chemistry and Biochemistry, Ruhr University Bochum, Universitätsstr. 150, D-44780 Bochum, Germany.

References

1. Breisch M, Grasmik V, Loza K, Pappert K, Rostek A, Ziegler N, Ludwig A, Heggen M, Epple M, Tiller JC, Schildhauer TA, Köller M, Sengstock C (2019) Bimetallic silver-platinum nanoparticles with combined osteo-promotive and antimicrobial activity. Nanotechnology 30:305101. https://doi.org/10.1088/1361-6528/ab172b
2. Conde J, Doria G, Baptista P (2012) Noble metal nanoparticles applications in cancer. J Drug Deliv 2012:751075. https://doi.org/10.1155/2012/751075
3. Weissleder R, Elizondo G, Wittenberg J, Rabito CA, Bengele HH, Josephson L (1990) Ultrasmall superparamagnetic iron oxide: characterization of a new class of contrast agents for MR imaging. Radiology 175:489–493. https://doi.org/10.1148/radiology.175.2.2326474
4. Li J, Zhang JZ (2009) Optical properties and applications of hybrid semiconductor nanomaterials. Coordination Chemistry Reviews, 253(23-24), 3015-3041. https://doi.org/10.1016/J.CCR.2009.07.017

5. Karmakar S, Kumar S, Rinaldi R, Maruccio G (2011) Nano-electronics and spintronics with nanoparticles. J. Phys.: Conf. Ser. 292:12002. https://doi.org/10.1088/1742-6596/292/1/012002
6. Astruc D (2008) Nanoparticles and catalysis. Wiley-VCH, Weinheim
7. Kharisov BI, Dias HR, Kharissova OV (2019) Mini-review: Ferrite nanoparticles in the catalysis. Arabian Journal of Chemistry 12:1234–1246. https://doi.org/10.1016/j.arabjc.2014.10.049
8. Migowski P, Dupont J (2007) Catalytic applications of metal nanoparticles in imidazolium ionic liquids. Chemistry 13:32–39. https://doi.org/10.1002/chem.200601438
9. Bracey CL, Ellis PR, Hutchings GJ (2009) Application of copper-gold alloys in catalysis: current status and future perspectives. Chem Soc Rev 38:2231–2243. https://doi.org/10.1039/b817729p
10. Garzón-Manjón A, Solano E, La Mata M de, Guzmán R, Arbiol J, Puig T, Obradors X, Yáñez R, Ricart S, Ros J (2015) Induced shape controllability by tailored precursor design in thermal and microwave-assisted synthesis of Fe3O4 nanoparticles. J Nanopart Res 17. https://doi.org/10.1007/s11051-015-3070-x
11. Garzón-Manjón A, Aranda-Ramos A, Melara-Benítez B, Bensarghin I, Ros J, Ricart S, Nogués C (2018a) Simple Synthesis of Biocompatible Stable CeO2 Nanoparticles as Antioxidant Agents. Bioconjug Chem 29:2325–2331. https://doi.org/10.1021/acs.bioconjchem.8b00300
12. Itoh H, Naka K, Chujo Y (2004) Synthesis of gold nanoparticles modified with ionic liquid based on the imidazolium cation. J Am Chem Soc 126:3026–3027. https://doi.org/10.1021/ja039895g
13. Raut D, Wankhede K, Vaidya V, Bhilare S, Darwatkar N, Deorukhkar A, Trivedi G, Salunkhe M (2009) Copper nanoparticles in ionic liquids: Recyclable and efficient catalytic system for 1,3-dipolar cycloaddition reaction. Catalysis Communications 10:1240–1243. https://doi.org/10.1016/j.catcom.2009.01.027
14. Sahoo P, Kamal S, Kumar T, Sreedhar B, Singh A, Srivastava S (2009) Synthesis of Silver Nanoparticles using Facile Wet Chemical Route. DSJ 59:447–455. https://doi.org/10.14429/dsj.59.1545
15. Yang H, Zhang J, Kumar S, Zhang H, Yang R, Fang J, Zou S (2009) Monodisperse and highly active PtNi nanoparticles for O2 reduction. Electrochemistry Communications 11:2278–2281. https://doi.org/10.1016/j.elecom.2009.10.009
16. Baraton M-I (ed) (2003) Synthesis, functionalization and surface treatment of nanoparticles. American Scientific Publ, Stevenson Ranch, Calif.
17. Datta MK, Pabi SK, Murty BS (2000) Phase fields of nickel silicides obtained by mechanical alloying in the nanocrystalline state. Journal of Applied Physics 87:8393–8400. https://doi.org/10.1063/1.373553
18. Lam C, Zhang YF, Tang YH, Lee CS, Bello I, Lee ST (2000) Large-scale synthesis of ultrafine Si nanoparticles by ball milling. Journal of Crystal Growth 220:466–470. https://doi.org/10.1016/S0022-0248(00)00882-4
19. Cui H, Feng Y, Ren W, Zeng T, Lv H, Pan Y (2009) Strategies of large scale synthesis of monodisperse nanoparticles. Recent Pat Nanotechnol 3:32–41. https://doi.org/10.2174/187221009787003302
20. Kim D-Y, Suk Sung J, Kim M, Ghodake G (2015) Rapid production of silver nanoparticles at large-scale using gallic acid and their antibacterial assessment. Materials Letters 155:62–64. https://doi.org/10.1016/j.matlet.2015.04.138
21. Lee Y, Lee J, Bae CJ, Park J-G, Noh H-J, Park J-H, Hyeon T (2005) Large-Scale Synthesis of Uniform and Crystalline Magnetite Nanoparticles Using Reverse Micelles as Nanoreactors under Reflux Conditions. Adv.

Funct. Mater. 15:503–509. https://doi.org/10.1002/adfm.200400187

22. Lee Y, Choi J-R, Lee KJ, Stott NE, Kim D (2008) Large-scale synthesis of copper nanoparticles by chemically controlled reduction for applications of inkjet-printed electronics. Nanotechnology 19:415604. https://doi.org/10.1088/0957-4484/19/41/415604
23. Lee C-C, Chen D-H (2006) Large-scale synthesis of Ni–Ag core–shell nanoparticles with magnetic, optical and anti-oxidation properties. Nanotechnology 17:3094–3099. https://doi.org/10.1088/0957-4484/17/13/002
24. Song H, Chen X (2003) Large-scale synthesis of carbon-encapsulated iron carbide nanoparticles by co-carbonization of durene with ferrocene. Chemical Physics Letters 374:400–404. https://doi.org/10.1016/S0009-2614(03)00773-5
25. Wen Y, Huang W, Wang B, Fan J, Gao Z, Yin L (2012) Synthesis of Cu nanoparticles for large-scale preparation. Materials Science and Engineering: B 177:619–624. https://doi.org/10.1016/j.mseb.2012.02.026
26. Athanassiou EK, Grass RN, Stark WJ (2006) Large-scale production of carbon-coated copper nanoparticles for sensor applications. Nanotechnology 17:1668–1673. https://doi.org/10.1088/0957-4484/17/6/022
27. Wang X, Huang Z, Yao Y, Qiao H, Zhong G, Pei Y, Zheng C, Kline D, Xia Q, Lin Z, Dai J, Zachariah MR, Yang B, Shahbazian-Yassar R, Hu L (2020) Continuous 2000 K droplet-to-particle synthesis. Materials Today 35:106–114. https://doi.org/10.1016/j.mattod.2019.11.004
28. Lu J, Yang J-x, Wang J, Lim A, Wang S, Loh KP (2009) One-pot synthesis of fluorescent carbon nanoribbons, nanoparticles, and graphene by the exfoliation of graphite in ionic liquids. ACS Nano 3:2367–2375. https://doi.org/10.1021/nn900546b
29. Xiao D, Yuan D, He H, Gao M (2013) Microwave assisted one-step green synthesis of fluorescent carbon nanoparticles from ionic liquids and their application as novel fluorescence probe for quercetin determination. Journal of Luminescence 140:120–125. https://doi.org/10.1016/j.jlumin.2013.02.032
30. Zheng W, Liu X, Yan Z, Zhu L (2009) Ionic liquid-assisted synthesis of large-scale TiO2 nanoparticles with controllable phase by hydrolysis of TiCl4. ACS Nano 3:115–122. https://doi.org/10.1021/nn800713w
31. Luska KL, Migowski P, Leitner W (2015) Ionic liquid-stabilized nanoparticles as catalysts for the conversion of biomass. Green Chem. 17:3195–3206. https://doi.org/10.1039/C5GC00231A
32. Plechkova NV, Seddon KR (2008) Applications of ionic liquids in the chemical industry. Chem Soc Rev 37:123–150. https://doi.org/10.1039/b006677j
33. Holbrey JD, Seddon KR (1999) Ionic Liquids. Clean Technologies and Environmental Policy 1:223–236. https://doi.org/10.1007/s100980050036
34. Kuwabata S, Torimoto T, Imanishi A, Tsu T (2014) Use of Ionic Liquid Under Vacuum Conditions. In: Kadokawa J-i (ed) Ionic liquids - new aspects for the future. InTech, Croatia, Japan
35. Wasserscheid P, Keim W (2000) Ionic Liquids—New “Solutions” for Transition Metal Catalysis. Angew. Chem. Int. Ed. 39:3772–3789. https://doi.org/10.1002/1521-3773(20001103)39:21<3772:AID-ANIE3772>3.0.CO;2-5

36. Vekariya RL (2017) A review of ionic liquids: Applications towards catalytic organic transformations. Journal of Molecular Liquids 227:44–60. https://doi.org/10.1016/j.molliq.2016.11.123
37. Torimoto T, Okazaki K-i, Kiyama T, Hirahara K, Tanaka N, Kuwabata S (2006) Sputter deposition onto ionic liquids: Simple and clean synthesis of highly dispersed ultrafine metal nanoparticles. Appl. Phys. Lett. 89:243117. https://doi.org/10.1063/1.2404975
38. Richter K, Birkner A, Mudring A-V (2010) Stabilizer-free metal nanoparticles and metal-metal oxide nanocomposites with long-term stability prepared by physical vapor deposition into ionic liquids. Angew. Chem. Int. Ed. 49:2431–2435. https://doi.org/10.1002/anie.200901562
39. Richter K, Birkner A, Mudring A-V (2011) Stability and growth behavior of transition metal nanoparticles in ionic liquids prepared by thermal evaporation: how stable are they really? Phys Chem Chem Phys 13:7136–7141. https://doi.org/10.1039/c0cp02623a
40. König D, Richter K, Siegel A, Mudring A-V, Ludwig A (2014) High-Throughput Fabrication of Au-Cu Nanoparticle Libraries by Combinatorial Sputtering in Ionic Liquids. Adv. Funct. Mater. 24:2049–2056. https://doi.org/10.1002/adfm.201303140
41. Hatakeyama Y, Okamoto M, Torimoto T, Kuwabata S, Nishikawa K (2009) Small-Angle X-ray Scattering Study of Au Nanoparticles Dispersed in the Ionic Liquids 1-Alkyl-3-methylimidazolium Tetrafluoroborate. J. Phys. Chem. C 113:3917–3922. https://doi.org/10.1021/jp807046u
42. Hirano M, Enokida K, Okazaki K-i, Kuwabata S, Yoshida H, Torimoto T (2013) Composition-dependent electrocatalytic activity of AuPd alloy nanoparticles prepared via simultaneous sputter deposition into an ionic liquid. Phys Chem Chem Phys 15:7286–7294. https://doi.org/10.1039/c3cp50816a
43. Meischein M, Garzón-Manjón A, Frohn T, Meyer H, Salomon S, Scheu C, Ludwig A (2019) Combinatorial Synthesis of Binary Nanoparticles in Ionic Liquids by Cosputtering and Mixing of Elemental Nanoparticles. ACS Comb Sci 21:743–752. https://doi.org/10.1021/acscombsci.9b00140
44. Meyer H, Meischein M, Ludwig A (2018) Rapid Assessment of Sputtered Nanoparticle Ionic Liquid Combinations. ACS Comb Sci 20:243–250. https://doi.org/10.1021/acscombsci.8b00017
45. Veith G, Lupini A, Pennycook S, Ownby G, Dudney N (2005) Nanoparticles of gold on γ-Al2O3 produced by dc magnetron sputtering. Journal of Catalysis 231:151–158. https://doi.org/10.1016/j.jcat.2004.12.008
46. Garzón-Manjón A, Meyer H, Grochla D, Löffler T, Schuhmann W, Ludwig A, Scheu C (2018b) Controlling the Amorphous and Crystalline State of Multinary Alloy Nanoparticles in An Ionic Liquid. Nanomaterials (Basel) 8. https://doi.org/10.3390/nano8110903
47. Löffler T, Meyer H, Savan A, Wilde P, Garzón Manjón A, Chen Y-T, Ventosa E, Scheu C, Ludwig A, Schuhmann W (2018) Discovery of a Multinary Noble Metal-Free Oxygen Reduction Catalyst. Adv. Energy Mater. 8:1802269. https://doi.org/10.1002/aenm.201802269
48. Meischein M, Fork M, Ludwig A (2020) On the Effects of Diluted and Mixed Ionic Liquids as Liquid Substrates for the Sputter Synthesis of Nanoparticles. Nanomaterials (Basel) 10. https://doi.org/10.3390/nano10030525
49. Meshesha BT, Barrabés N, Medina F, Sueiras J Polyol mediated synthesis & characteritzation of Cu nanoparticles: Effect of 1-hexadecylamine as stabilizing agent. In: Proceedings of the 1st WSEAS international conference on Nanotechnology, pp 87–91

50. Salas G, Podgoršek A, Campbell PS, Santini CC, Pádua AAH, Costa Gomes MF, Philippot K, Chaudret B, Turmine M (2011) Ruthenium nanoparticles in ionic liquids: structural and stability effects of polar solutes. Phys Chem Chem Phys 13:13527–13536. https://doi.org/10.1039/c1cp20623k
51. Zhang S, Zhang Y, Wang Y, Liu S, Deng Y (2012) Sonochemical formation of iron oxide nanoparticles in ionic liquids for magnetic liquid marble. Phys Chem Chem Phys 14:5132–5138. https://doi.org/10.1039/c2cp23675c
52. Qadir MI, Weilhard A, Fernandes JA, Pedro I de, Vieira BJC, Waerenborgh JC, Dupont J (2018) Selective Carbon Dioxide Hydrogenation Driven by Ferromagnetic RuFe Nanoparticles in Ionic Liquids. ACS Catal. 8:1621–1627. https://doi.org/10.1021/acscatal.7b03804
53. Qadir MI, Bernardi F, Scholten JD, Baptista DL, Dupont J (2019) Synergistic CO2 hydrogenation over bimetallic Ru/Ni nanoparticles in ionic liquids. Applied Catalysis B: Environmental 252:10–17. https://doi.org/10.1016/j.apcatb.2019.04.005
54. Dash P, Scott RWJ (2009) 1-Methylimidazole stabilization of gold nanoparticles in imidazolium ionic liquids. Chem Commun (Camb):812–814. https://doi.org/10.1039/B816446K

Figures

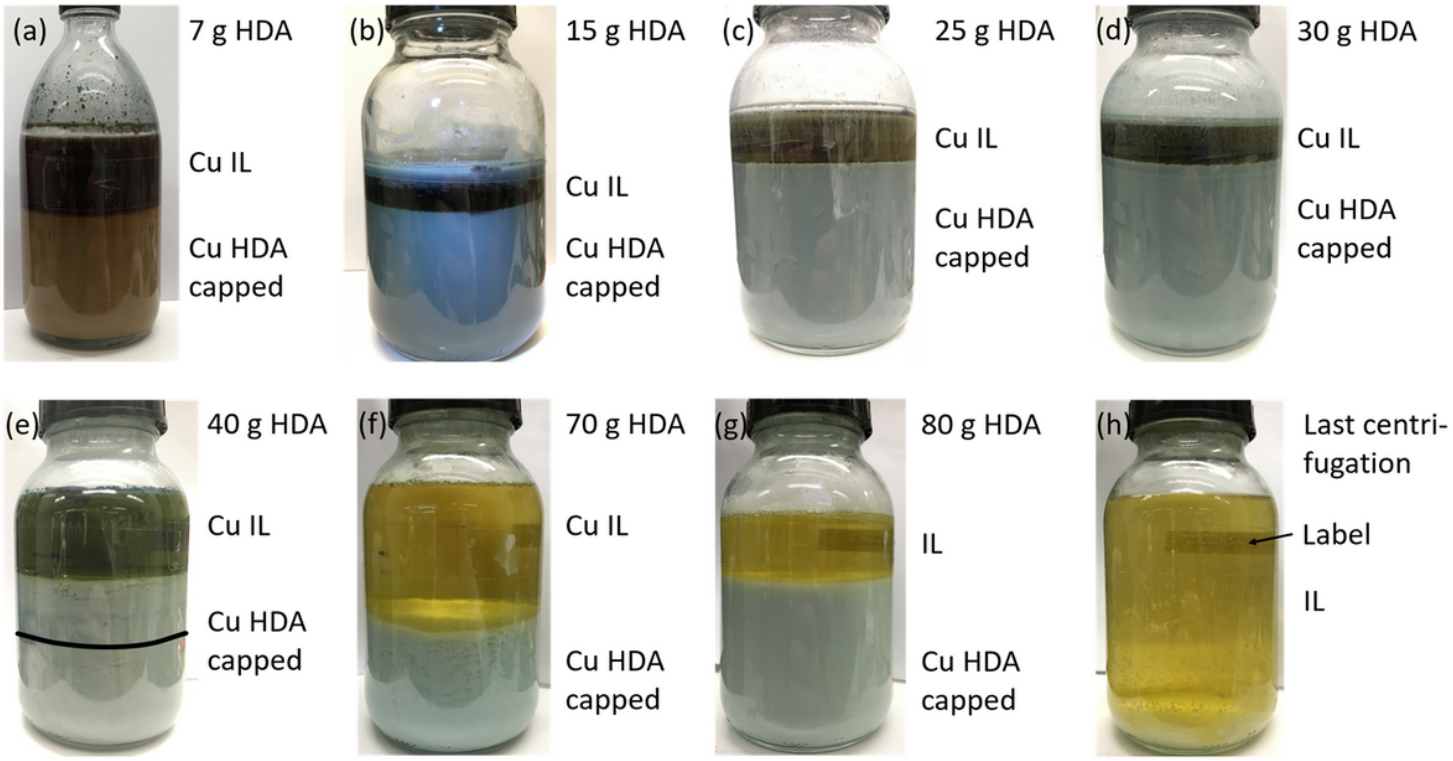

Figure 1

Different stages of the NP capping process. The amount of HDA-capped NPs increases with the increasing amount of used HDA which is 7 g in (a), 15 g in (b), 25 g in (c), 30 g in (d), 40 g in (e), 70 g in (f) and 80 g in (g). Between the HDA addition from 7 g to 15 g a bigger bottle had to be used since the volume of capped NPs with the necessary HDA and acetonitrile addition would have exceeded the volume of the smaller bottle.

Between images (d) and (e) approximately half of the capped Cu NPs was used for the first centrifugation session after reaching 35 g of HDA in total. The black line in (e) shows the level of remaining HDA capped Cu NPs after the extraction of the NP material. In (h) the remaining liquid after the 6th centrifugation round is shown. The transparency (note the label which is positioned at the back wall of the bottle) indicates that the NPs were extracted from the IL to a very high degree.

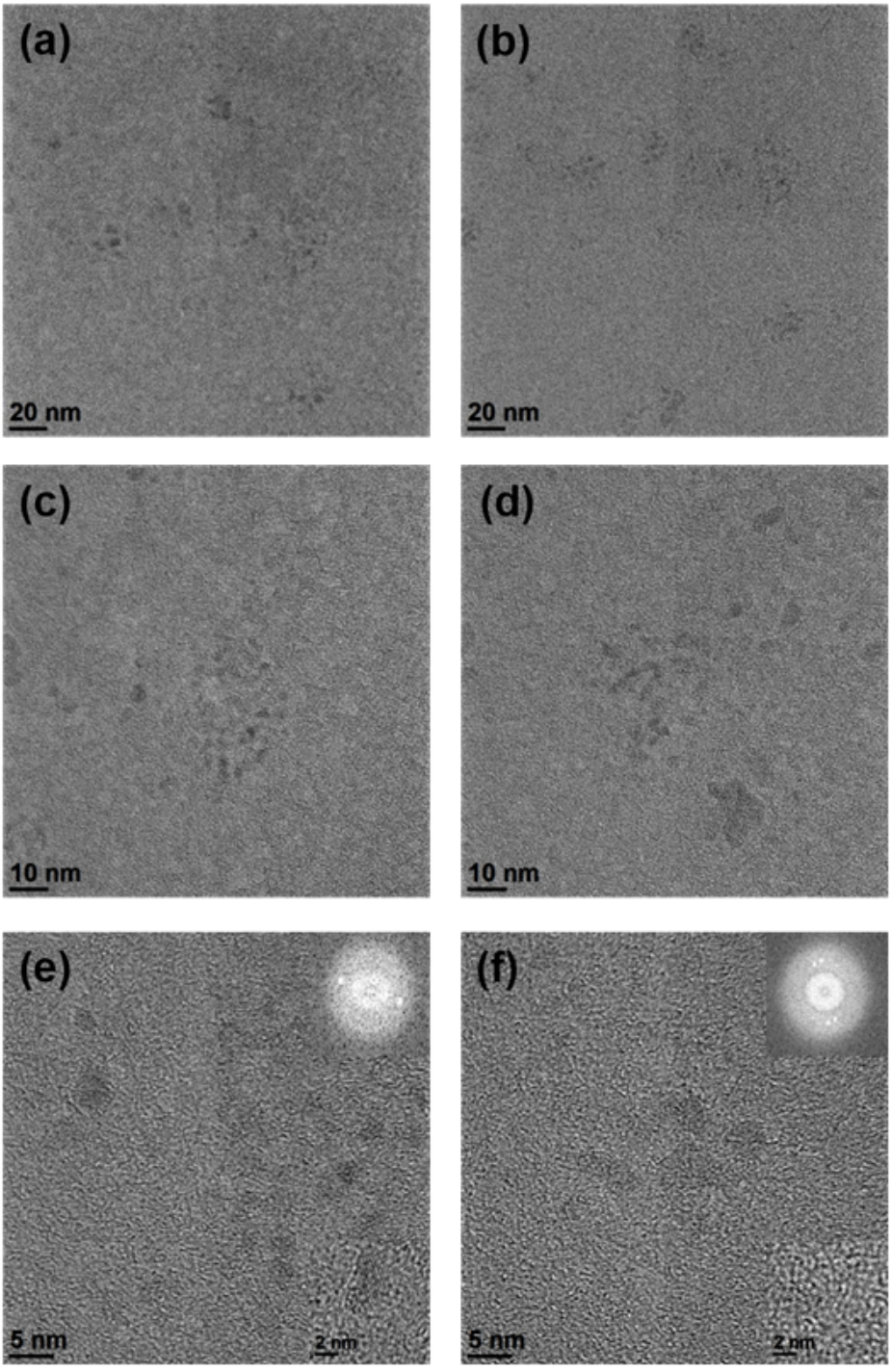

Figure 2

Overview of the NPs from the as prepared up-scaled-synthesized Cu IL directly after the deposition. The Cu NPs are organized mainly in loosely bounded agglomeration structures with individual NPs. Crystallinity was

detected as depicted in the close-up NP image insets and the corresponding FFT graphs in the insets in (e) and (f).

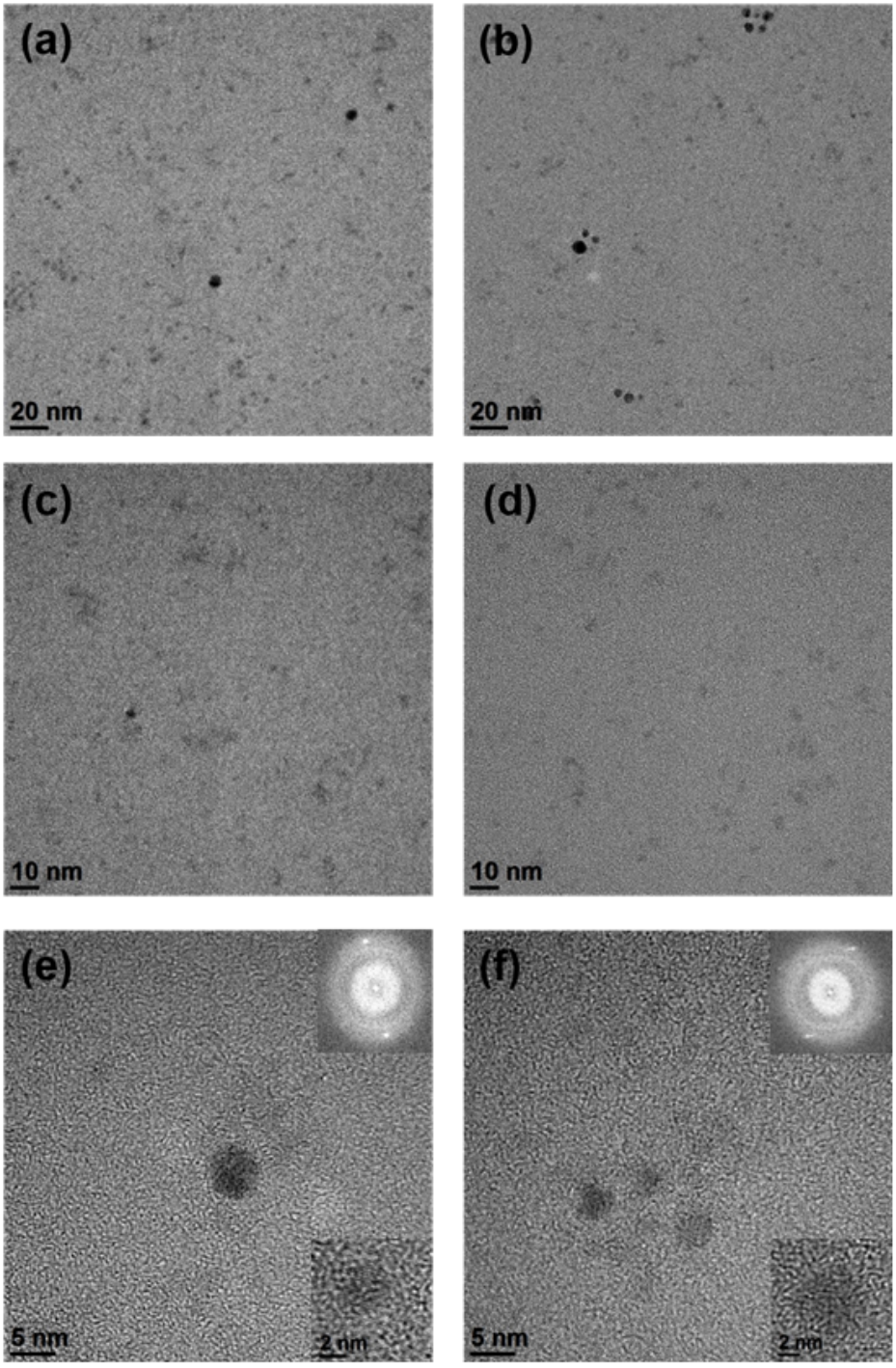

Figure 3

Overview of NPs from the as prepared Cu IL synthesized for scientific purposes directly after deposition. Crystallinity was detected as depicted in the close-up NP image insets and the corresponding FFT graphs in the insets in (e) and (f).

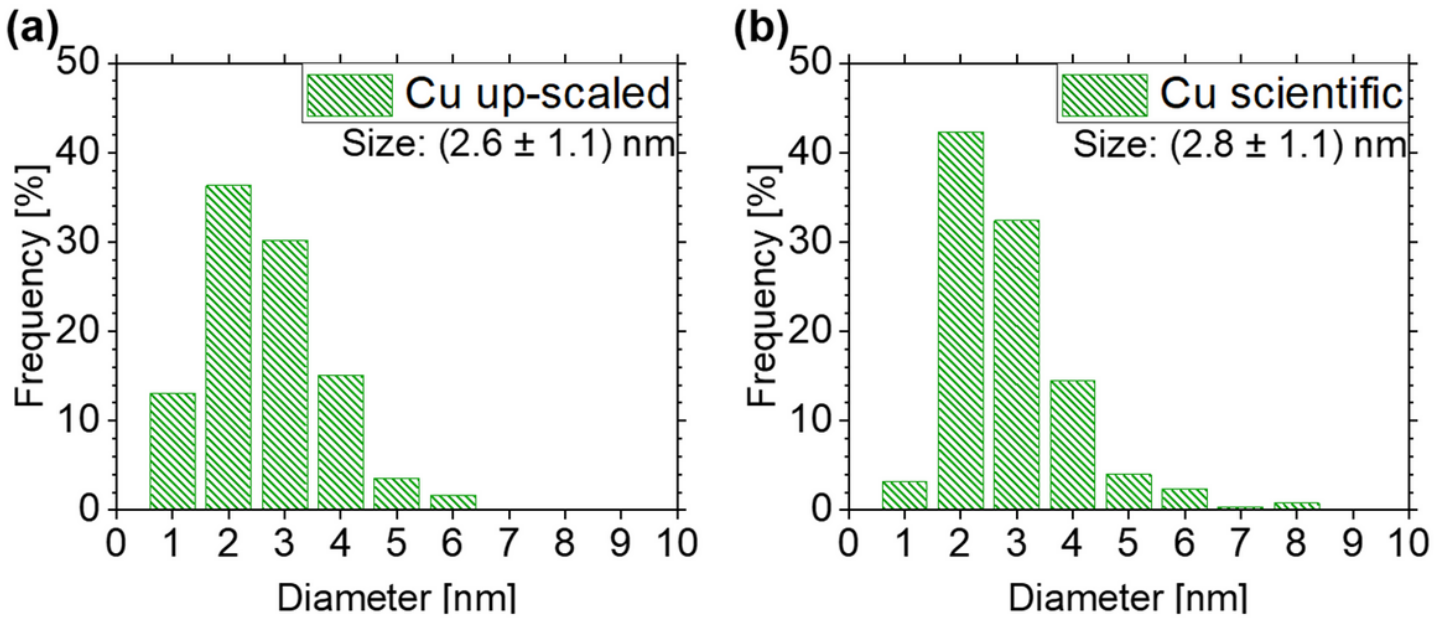

Figure 4

NP size distributions for both types of Cu NP in IL depositions. The NP size distribution of the up-scaled Cu deposition is shown in (a) and the size distribution of the NPs obtained from the scientific deposition is depicted in (b). Both size distributions show a comparable spread of the NP diameters with the NPs from the scientific deposition being slightly bigger and a maximum NP size exceeding the maximum NP size obtained from the up-scaled Cu deposition.

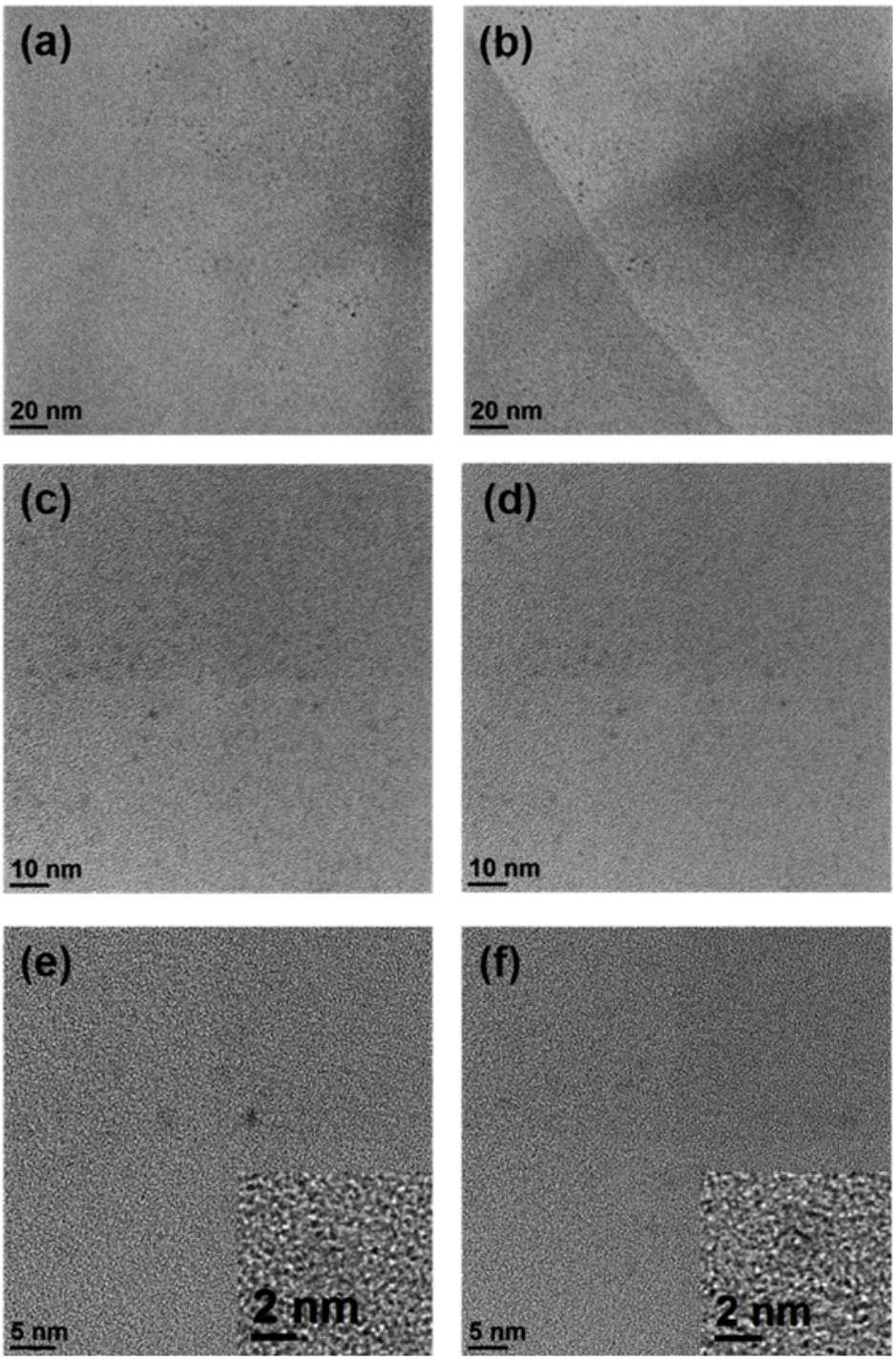

Figure 5

Overview of the HDA-capped Cu NPs dissolved in toluene prior to the TEM grid preparation. Compared to the as-prepared Cu NPs, the HDA-capped NPs are not organized in agglomerated structures but are well distributed.

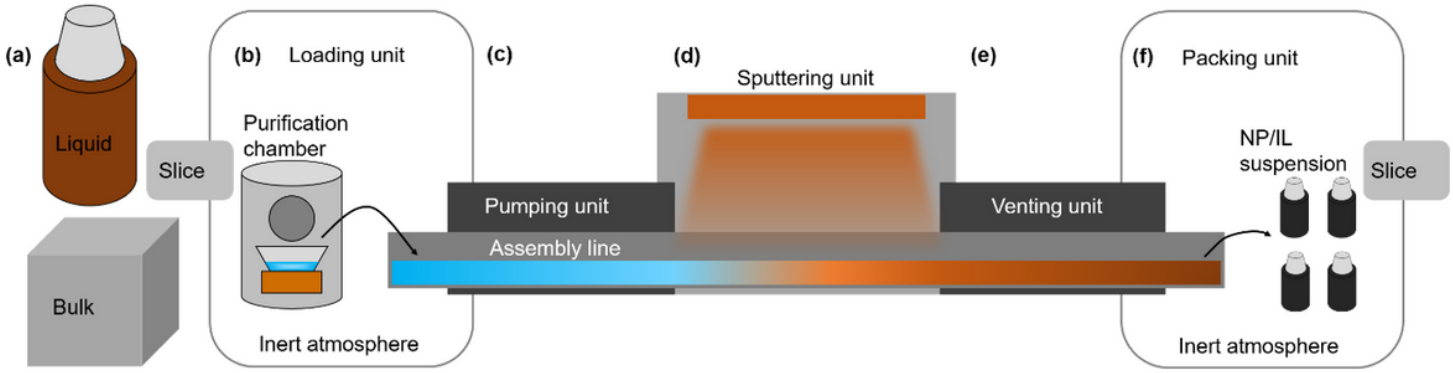

Figure 6

Schematic illustration of a possible upscaling production line for NP/IL. IL can be delivered in liquid or bulk state in (a) and introduced into the loading unit (b) with inert atmosphere. The IL can be purified within the loading unit, e.g. by annealing at mild temperatures below 100°C within slight vacuum and then loaded onto the assembly line. The assembly line is pumped at different pumping stages in (c) until the sputter pressure is reached. The sputter unit (d) is directly attached to the pumping unit. The sputtered IL is transported back to atmospheric pressure via the venting unit (e) using inert atmosphere. The vented assembly line ends in the packing unit (f) also among inert atmosphere where the NP/IL suspension is packed or transported to its further applications.